https://doi.org/10.5194/acp-2022-282
Preprint. Discussion started: 18 May 2022

Atmospheric Chemistry and Physics Discussions

Detection of Stratospheric Air Intrusion Events From Ground-based High-resolution $^{10}Be/^{7}Be$ by Accelerator Mass Spectrometry

Xu-Ke Liu[1,2,3,5,#], Yun-Chong Fu[1,2,4,#,*], Li Zhang[1,2], George S. Burr[1], Yan-Ting Bi[5], Guo-Qing Zhao[1,2]

1. State Key Laboratory of Loess and Quaternary Geology, Institute of Earth Environment, Chinese Academy of Sciences (IEECAS), Xi'an 710061, China

2. Shaanxi Key Laboratory of Accelerator Mass Spectrometry Technology and Application, Xi'an AMS Center of IEECAS, Xi'an 710061, China

3. University of Chinese Academy of Sciences, Beijing 100049, China

4. Institute of Global Environmental Change, Xi'an Jiaotong University, Xi'an 710049, China

5. Xi'an Institute for Innovative Earth Environment Research, Xi'an, 710061, China

#The authors contribution equally to this work and should be considered co-first authors

**Corresponding author: Yun-Chong Fu, E-mail: fuyc@ieecas.cn.*

Abstract

Locally rapid stratospheric air intrusions facilitate the transport of stratospheric material to the troposphere. Long-term continuous monitoring of such events by traditional techniques, such as sounding technology, is challenging. Beryllium-7 (^{7}Be) and beryllium-10 (^{10}Be) offer an alternative. These isotopes are formed by cosmic rays and are mainly produced in the lower stratosphere and upper troposphere. Due to their similar geochemical properties and substantial difference in half-lives favor relatively high $^{10}Be/^{7}Be$ ratios in the stratosphere, as compared to the troposphere. Monitoring surface $^{10}Be/^{7}Be$ ratios affords a potential means to identify stratospheric air intrusions. However, high temporal resolution $^{10}Be/^{7}Be$ observational records must be taken and corrected for dust-borne ^{10}Be to identify stratospheric air intrusions. In

https://doi.org/10.5194/acp-2022-282
Preprint. Discussion started: 18 May 2022

Atmospheric Chemistry and Physics Discussions

this study, we use Accelerator Mass Spectrometry to measure both ^{7}Be and ^{10}Be in rain and aerosol (down to ~ 200 cubic meters air) with an error of ~ 1.5%. We correct for dust-borne ^{10}Be using soil Al. This method provides precise measurements with daily resolution. We present annual beryllium isotopes (^{7}Be, ^{10}Be, and ^{10}Be/^{7}Be ratio) record for the Chinese Loess Plateau that includes several regional sites. We show that for the city of Xi'an, the proportion of dust-borne (resuspended) ^{10}Be was ~24% in 2020/21. Our results confirm that stratospheric air intrusion events in the Loess Plateau are frequent and rapid throughout the year and are strongest in the spring (March-July), when ^{10}Be/^{7}Be values were observed to increase about a factor of 3. Even in winter, weaker stratospheric air intrusion events can be detected. Calculated $\Delta(^{10}Be/^{7}Be)$ values in winter suggest stratospheric ozone transport can lead to an ~25% cumulative increase the surface ozone.

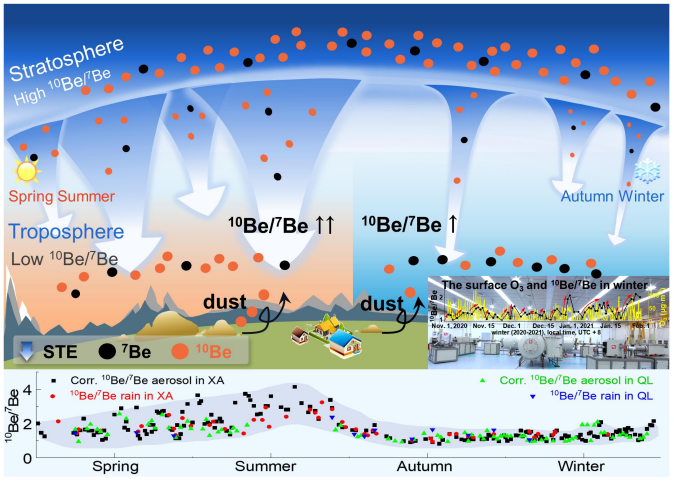

Abstract graph

Key words: Cosmogenic nuclides, Stratospheric air intrusion, ^{10}Be/^{7}Be ratio,

https://doi.org/10.5194/acp-2022-282
Preprint. Discussion started: 18 May 2022


Atmospheric Chemistry and Physics Discussions

42 Accelerator mass spectrometry, Ozone transport, Loess Plateau

43

44 **1. Introduction**

45 Stratospheric air intrusions are a vital process in stratosphere-troposphere
46 exchange (STE), providing a transport mechanism for stratospheric materials to the
47 ground (Holton et al., 1995;Randel et al., 2010). Local stratospheric air intrusions are
48 difficult to quantify and may have hard-to-capture frequent intrusion events
49 (Hodnebrog et al., 2016;Sudo et al., 2003). Although these local stratospheric air
50 intrusions are relatively weak, they can still facilitate the transport of natural and
51 anthropogenic trace chemicals and significantly affects the atmospheric chemistry,
52 atmospheric heat budget, and radiation properties. For example, stratospheric air
53 intrusions can facilitate ozone (O_3) transport to the troposphere (Baylon et al., 2016).
54 Tropospheric O_3 affects human health and ecological environments. Due to the
55 scarcity of observational data in the lower stratosphere and upper troposphere, there
56 are few observational studies on this process. Traditional observation methods of
57 stratospheric air intrusion mainly rely on sounding technology with multi-element
58 sensors (Fischer et al., 2008). However, the observation process is complicated, and it
59 is challenging to observe continuously due to the influence of weather, let alone
60 accurate capture of frequent intrusion events in local areas.

61 Meteoric ^{7}Be and ^{10}Be are produced by cosmic rays interacting with oxygen and
62 nitrogen, mainly in the lower stratosphere and upper troposphere (Brown et al., 1989).
63 After their formation, these beryllium isotopes are rapidly absorbed and transported

https://doi.org/10.5194/acp-2022-282
Preprint. Discussion started: 18 May 2022


Atmospheric Chemistry and Physics Discussions

by submicron aerosols (Lal et al., 1958), and it is generally believed that ground-based ^{7}Be analyses offer a means of identifying and tracing stratospheric air intrusions (Bhandari et al., 1966;Hernandez-Ceballos et al., 2017). Using ^{7}Be alone is complicated by tropospheric weather conditions and the latitudinal dependence of ^{7}Be production at different latitudes (Masarik and Beer, 1999). Using ^{10}Be/^{7}Be ratios can avoid these effects, making it more accurate and sensitive than ^{7}Be concentrations alone to trace stratospheric air intrusions (Jordan et al., 2003). The transport and deposition processes of ^{7}Be and ^{10}Be are same, and their production rates ratio at each latitude is consistent (Masarik and Beer, 1999). The two isotopes have different residence times in the stratosphere and troposphere and the very different half-lives: ^{7}Be ($T_{1/2}$ = 53.29 d) and ^{10}Be ($T_{1/2}$ = 1.36 Ma). These factors make stratospheric ^{10}Be/^{7}Be ratios much larger than ^{10}Be/^{7}Be ratios observed near the surface air (Jordan et al., 2003). When stratospheric air intrudes, the ^{10}Be/^{7}Be ratio in the atmosphere at the earth's surface increases (Brown et al., 1989).

^{7}Be and ^{10}Be are typically measured by gamma spectrometry and accelerator mass spectrometry (AMS), respectively. Due to the low counting efficiency of the gamma spectrometry, large samples are required (> 10^{3} m^{3} air or > 10 L rain), as well as lengthy measurements (> 1 day) to obtain optimal measurement uncertainties (Tiessen et al., 2019;Yamagata et al., 2019). It is even more challenging to obtain ^{7}Be data with low uncertainty at a daily resolution based on gamma spectrometry, especially in short-period field sampling and quickly stratospheric air intrusion event research. Measuring ^{7}Be by AMS significantly reduces sample size requirements and

https://doi.org/10.5194/acp-2022-282
Preprint. Discussion started: 18 May 2022


Atmospheric Chemistry and Physics Discussions

improves the detection limit by approximately 10-100 times (Raisbeck and Yiou, 1988). Hence, we measure both isotopes with AMS.

Due to the high abundance of ^{10}Be in topsoil, resuspended dust-borne ^{10}Be must be accounted (Czymzik et al., 2018;Yamagata et al., 2010). In particular, corrections are necessary for STE studies in high dust areas such as the Chinese Loess Plateau (one of the leading dust source areas in Asia (Zhang et al., 1997)), that reflect ^{10}Be/^{7}Be from dry deposition (Heikkila et al., 2013). We have devised a means of making these corrections based in part on our previous studies of ^{10}Be in loess (Beck et al., 2018). In addition, high-precision ^{7}Be and ^{10}Be data can contribute to our understanding of atmospheric material transport and circulation (Chham et al., 2019;Liu et al., 2022), solar variability (Adolphi et al., 2014), and paleoclimate (Beck et al., 2018).

In this work, we use ground-based ^{10}Be/^{7}Be measurements as a means of documenting stratospheric air intrusion events through time. In order to achieve this, we first developed an AMS measurement method to quantify ^{7}Be and ^{10}Be together (named ^{7}Be-^{10}Be-AMS). Next, we identified an analytical means to remove the resuspended dust-borne ^{10}Be component, ultimately enabling the acquisition of ^{10}Be/^{7}Be records with low uncertainty and high temporal resolution in various environments. We made numerous analyses of aerosol and rain samples (n = 398) from the Loess Plateau, and an annual ^{10}Be/^{7}Be record with the daily resolution was obtained for the first time. We show a relationship between these stratospheric air intrusions in winter with surface O_3.

https://doi.org/10.5194/acp-2022-282
Preprint. Discussion started: 18 May 2022


Atmospheric Chemistry and Physics Discussions

2. Methods

2.1 Sample collection

From May 2020 to June 2021, aerosol and rainwater samples from multiple locations were collected. These sampling points include (Fig. S1): Xi'an (XA, 34°13′20″N, 109°00′18″E) and Qinling (QL, 34°3′43″N, 108°20′48″E) for long-term monitoring. Zhongwei (ZW, 37°30′57″N, 105°11′8″E), Taiyuan (TY, 37°48′26″N, 112°34′55″E), Chengdu (CD, 30°56′44″N, 103°40′41″E), Nanning (NN, 22°50′18″N, 108°16′51″E), and Lianyungang (LYG, 34°46′4″N, 119°26′55″E) for short-term intermittent monitoring. Aerosols and rainwater were collected at XA and QL, while only aerosols were collected at the remaining sampling sites.

Total suspended particulate (TSP) samples passed through a large-flow particle collector (TH-1000CII, Wuhan Tianhong Instrument. Co., Ltd.) and a portable small-flow particle collector (TH-150H, Wuhan Tianhong Instrument. Co., Ltd.), prior to collection on polypropylene filter membranes. Each collection period was 24 h and sampled approximately 200-500 m^3 air. For rain sample collection, the initial rainfall in the first half-hour was removed to avoid interference from suspended dust. Rainwater samples were collected and stored separately in acidified polyethylene containers to prevent beryllium in the rainwater from adsorbing on the container walls. Detailed rain sample collection information is described elsewhere (Zhang and Fu, 2017). Among multiple sampling points, the meteorological data collector (HOBO-U30 Station) established at the XA sampling site was used to accurately monitor meteorological data such as wind speed, precipitation, and solar radiation

https://doi.org/10.5194/acp-2022-282
Preprint. Discussion started: 18 May 2022


Atmospheric Chemistry and Physics Discussions

intensity. Surface O_3 concentration data at the XA site was downloaded from the government website https://www.aqistudy.cn/. The sampling times provided in this article are based on local time (UTC+8).

2.2 Extraction of Be and Al in the sample and preparation of the BeO target

^{7}Be and ^{10}Be targets were prepared according to established experimental procedures for loess ^{10}Be (Zhou et al., 2007), and rainwater ^{7}Be and ^{10}Be (Zhang and Fu, 2017). The existing experimental process for aerosol samples followed 3 steps (Fig. S2): 1) ^{7}Be and ^{10}Be extraction; 2) ion-exchange separation and purification; and 3) BeO preparation. The first step removes organic at 600 ℃, and the remaining aerosol component is dissolved in acid. Next, $Be(OH)_2$ is obtained by reaction with a weak base ($NH_3 \cdot H_2O$), and the precipitate is oxidized to BeO at 900 ℃. The Al content of aerosols extracted by acid immersion was measured by ICP-AES (ULTIMA-2, HORIBA Jobin Yvon, France) according to the method proposed by Yamagata et al. (2010).

2.3 AMS analysis of ^{7}Be and ^{10}Be

^{7}Be and ^{10}Be were analyzed in the same target by the 3 MV multi-nuclide AMS at the Xi'an Accelerator Mass Spectrometry Center, Institute of Earth Environment, Chinese Academy of Sciences. The analysis method follows the approach we established in 2017 (Zhang and Fu, 2017), with some subsequent refinements. In particular, the transmission efficiency after the second stripping foil was substantially improved, reaching approximately 24%, which greatly improved the total transmission efficiency and further improved the analysis precision. $^{10}Be^{4+}$ or $^{7}Be^{4+}$

https://doi.org/10.5194/acp-2022-282
Preprint. Discussion started: 18 May 2022


Atmospheric Chemistry and Physics Discussions

were analyzed in a gas ionization detector (energy spectrum shown in Fig. S3). Measurement details are given in the Methods section of the Supplementary Information.

Data quality was assessed considering chemical preparation, measurement uncertainties, and parallel sample monitoring results. A threshold sample recovery rate for the chemical treatment process is maintained at > 80%. Each measurement batch included a standard sample and a blank sample. Standard samples were used for calibration, and blank samples were used for monitoring procedures. The results for the blank samples were well below measured sample values (~10^3 times). The measurement results of parallel samples are consistent within 1σ (Table S1).

AMS ^{7}Be measurements were cross-checked by gamma spectrometry. Large samples (approximately 2000 m^3 air) were collected, and polypropylene membranes with high aerosol concentrations were selected for comparison. About 1/4 of them were analyzed by ^{7}Be-AMS. The ^{7}Be in the remaining 3/4 filter membranes were measured using a high purity germanium (HpGe) detector. The results show that the AMS results were consistent with the measurement HpGe detector results (Table S2). Furthermore, for the same samples, the uncertainties for samples measured by AMS were uniformly lower than those measured by HpGe detector (detailed measurement information of the HpGe detector is included in the support information).

2.4 Quantification of the resuspended dust contribution to ^{10}Be

The resuspended dust-borne ^{10}Be contribution was corrected as: $[^{10}Be]_{corr} = [^{10}Be]_{bulk} - [^{10}Be]_{dust}$. The dust proportion was estimated from the

https://doi.org/10.5194/acp-2022-282
Preprint. Discussion started: 18 May 2022


Atmospheric Chemistry and Physics Discussions

aluminum content $P = \frac{[Al]_{aerosol}}{Eff \cdot [Al]_{soil}}$, and this value was used to calculate the dust component from the soil ^{10}Be: $[^{10}Be]_{dust} = P \cdot [^{10}Be]_{soil}$ (Yamagata et al., 2010):

$$[^{10}Be]_{corr} = [^{10}Be]_{bulk} - \frac{[Al]_{aerosol}}{Eff \cdot [Al]_{soil}} \cdot [^{10}Be]_{soil} \quad (1)$$

where $[Al]_{aerosol}$ is the aerosol Al concentration extracted by acid dissolution ($g \cdot m^{-3}$). Eff is the acid leaching efficiency of Al in aerosols, which is 51% (Yamagata et al., 2010), as determined by comparisons between leached samples analyzed by ICP-AES and a large number of samples analyzed by NAA. $[Al]_{soil}$ is the Al content of the topsoil (wt%); $[^{10}Be]_{soil}$ is the ^{10}Be concentration of the topsoil ($atoms \cdot g^{-1}$).

For $[^{10}Be]_{soil}$ in equation (1), XA, QL, and TY belong to the Loess Plateau. According to our previous results, this value is $2.13 \cdot 10^8$ $atoms \cdot g^{-1}$ (Zhou et al., 2007). According to survey results of ^{10}Be in topsoil (Yi et al., (2019b) (Fig. S1), the $[^{10}Be]_{soil}$ values of ZW, LYG, CD, and NN are $11.70 \cdot 10^8$ $atoms \cdot g^{-1}$, $3.75 \cdot 10^8$ $atoms \cdot g^{-1}$, $4.45 \cdot 10^8$ $atoms \cdot g^{-1}$, and $2.50 \cdot 10^8$ $atoms \cdot g^{-1}$, respectively. The $[Al]_{soil}$ contents are 7.41 wt% (Xiong et al., 2010), 7.57 wt% (Qiu et al., 2014), 8.32 wt% (Tan et al., 2013), and 10.50 wt% (Qiu et al., 2014) on the Loess Plateau, LYG, CD, and NN, respectively.

Researchers have shown that removing the initial precipitation (the first half-hour) for rain samples reduces the resuspended dust-borne ^{10}Be (Graham et al., 2003) and allows for a straightforward estimation of ^{10}Be from wet deposition. However, in this approach, the particles associated with the STE source are discarded, obscuring the relationship with aerosol ^{10}Be. Therefore, to verify our dust-borne ^{10}Be

https://doi.org/10.5194/acp-2022-282
Preprint. Discussion started: 18 May 2022


Atmospheric Chemistry and Physics Discussions

corrections, we compare $^{10}Be/^{7}Be$ of aerosols and precipitation.

3. Results and discussion

3.1 Observations of atmospheric ^{7}Be and ^{10}Be deposited on the Chinese Loess Plateau

Measured atmospheric and rainwater ^{7}Be and ^{10}Be concentrations, and $^{10}Be/^{7}Be$ ratios from the XA and QL sites (May 2020 to June 2021) are presented in Fig. 1. At the XA site, the average annual aerosol ^{7}Be concentration was $(3.80 \pm 0.06)\cdot10^{4}$ atoms$\cdot m^{-3}$, and the average annual aerosol ^{10}Be concentration was $(8.09 \pm 0.13)\cdot10^{4}$ atoms$\cdot m^{-3}$. XA rainwater ^{7}Be values averaged $(4.00 \pm 0.16)\cdot10^{4}$ atoms$\cdot g^{-1}$, and ^{10}Be values averaged $(6.42 \pm 0.26)\cdot10^{4}$ atoms$\cdot g^{-1}$. At the QL site (Fig. 1b), the average annual aerosol ^{7}Be concentration was $(4.08 \pm 0.07)\cdot10^{4}$ atoms$\cdot m^{-3}$, and the average annual aerosol ^{10}Be concentration was $(6.76 \pm 0.11)\cdot10^{4}$ atoms$\cdot m^{-3}$. QL rainwater ^{7}Be values averaged $(4.86 \pm 0.19)\cdot10^{4}$ atoms$\cdot g^{-1}$, and ^{10}Be values averaged $(6.35 \pm 0.24)\cdot10^{4}$ atoms$\cdot g^{-1}$. The average annual $^{10}Be/^{7}Be$ ratio for XA was 2.22 ± 0.12, and the average for the ZQL site was 1.62 ± 0.08 (Fig. 1c). The complete dataset is given in Tables S3 and S4.

The XA sampling site is a typical high-dust locality on the Loess Plateau, and the QL sampling site is relatively humid with lower dust content. Both sites experience distinct similar seasonal changes. ^{7}Be and ^{10}Be aerosol concentrations show large fluctuations associated with precipitation (Fig. 1a, 2b). The ^{10}Be concentrations and $^{10}Be/^{7}Be$ ratio from dry deposition at the XA site are significantly higher than those at the QL site, as well as coastal areas near the same latitude during the same period

https://doi.org/10.5194/acp-2022-282
Preprint. Discussion started: 18 May 2022


Atmospheric Chemistry and Physics Discussions

(such as Dazaifu and Tokyo in Japan (Yamagata et al., 2019)), especially in the dry season of the Loess Plateau, such as spring. QL serves as a control site with relatively higher precipitation and is located in the Qinling National Nature Reserve with a high normalized vegetation index (NDVI) (He et al., 2019). QL is only 60 km away from XA. As shown in Fig. 1c, the $^{10}Be/^{7}Be$ ratio of dry and wet deposition at the two sampling sites during wet periods is consistent and reflects the amount of deposition. Aerosol $^{10}Be/^{7}Be$ ratios at the two sites during dry periods are higher than the rainwater $^{10}Be/^{7}Be$ from the same period. This phenomenon is more obvious at dusty XA than at QL. Fig. 1d shows that the mean TSP concentration at XA (234.20 $\mu g \cdot m^{-3}$) was higher than the mean at QL (119.94 $\mu g \cdot m^{-3}$). The average aerosol Al content at XA (3.6 $\mu g \cdot m^{-3}$) is significantly higher than at QL (1.5 $\mu g \cdot m^{-3}$) and in coastal areas (the mean in Japan is approximately 2.31 $\mu g \cdot m^{-3}$ (Yamagata et al., 2010)), which confirms that dust from the XA site has a higher probability of re-suspension.

XA is located in a warm temperate area with a semi-humid and semi-arid continental monsoon climate. Its rainy seasons are unevenly distributed, and the annual average precipitation is 500-750 mm (Chen et al., 2020b). The East Asian winter monsoon and high-altitude westerly jets that carry dust from the western and northern deserts profoundly impact the supply of aeolian materials on the Loess Plateau (Shen et al., 2010). Dust-borne ^{10}Be from resuspended soil dust contributes significantly to the surface aerosol ^{10}Be, and obscures atmospheric mass movement information such as the STE (Fig. 1a-c). As expressed in equation (1), to obtain the actual deposition flux and associated ^{10}Be and $^{10}Be/^{7}Be$, it is necessary to remove

https://doi.org/10.5194/acp-2022-282
Preprint. Discussion started: 18 May 2022

Atmospheric Chemistry and Physics Discussions

239 dust-borne interference, as discussed below.

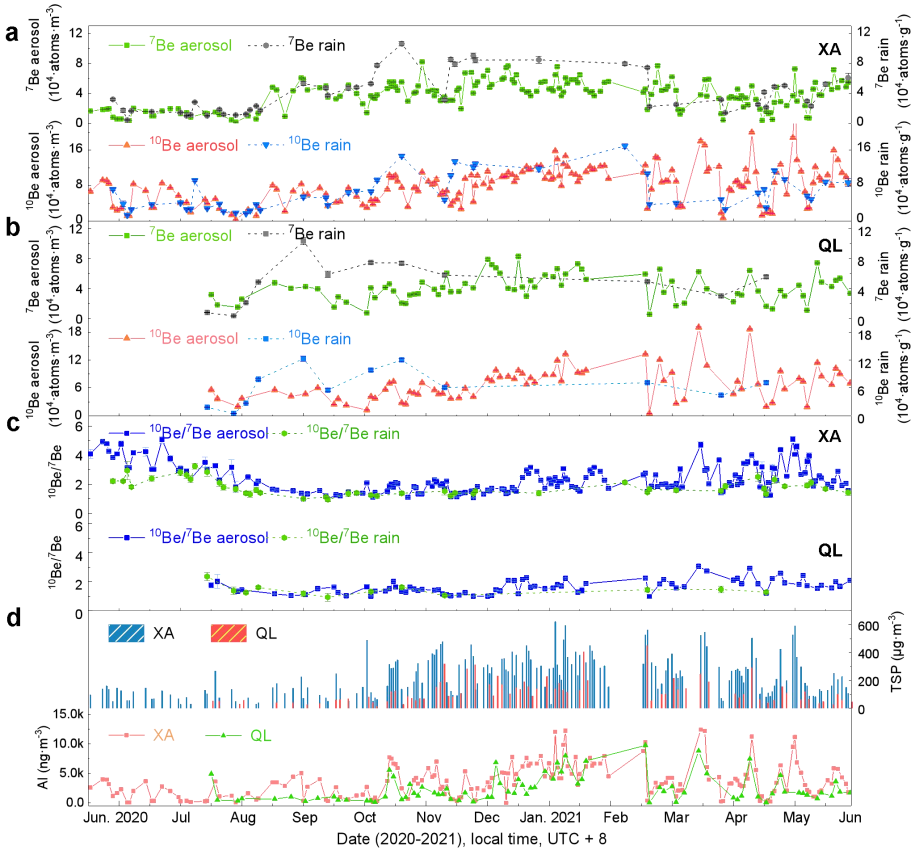

240

241 **Fig. 1** ^{7}Be and ^{10}Be concentrations and ^{10}Be/^{7}Be ratios in the atmosphere above the
242 Loess Plateau. Daily variation in ^{7}Be and ^{10}Be concentrations at XA (a) and at QL (b).
243 (c). Daily ^{10}Be/^{7}Be ratios (wet and dry deposition) of the Loess Plateau. (d). Daily
244 atmospheric TSP content and aerosol Al content at XA and QL.

245

246 **3.2 Correction for dust-borne ^{10}Be on aerosol ^{10}Be/^{7}Be values**

247 Due to its long half-life (1.36×10^{6} years), ^{10}Be accumulates after being deposited
248 on the ground, and ^{10}Be abundances per gram of soil are approximately 10^{4} times

https://doi.org/10.5194/acp-2022-282
Preprint. Discussion started: 18 May 2022


Atmospheric Chemistry and Physics Discussions

249 higher than corresponding ^{10}Be abundances in the near-ground atmosphere. In
250 contrast, ^{7}Be can not accumulate in the soil due to its relatively short half-life (53.3
251 days) (Yamagata et al., 2010). Therefore, resuspended dust-borne ^{10}Be can increase
252 the atmospheric ^{10}Be concentration and ^{10}Be/^{7}Be ratios. Dust-borne ^{10}Be can be
253 corrected by considering all of the sources of ^{10}Be in the bulk measurements:

254 $$[^{10}Be]_{bulk} = [^{10}Be]_{bg} + [^{10}Be]_{STE} + [^{10}Be]_{dust} \quad (2)$$

255 $$[^{10}Be]_{corr} = [^{10}Be]_{bg} + [^{10}Be]_{STE} \quad (3)$$

256 The measured aerosol ^{10}Be concentration, $[^{10}Be]_{bulk}$ contains three distinct ^{10}Be
257 components (equation 2). The background value $[^{10}Be]_{bg}$ refers to the ^{10}Be
258 concentration in the surface-atmosphere at equilibrium with no STE component.
259 $[^{10}Be]_{STE}$ is the ^{10}Becarried by the STE, and $[^{10}Be]_{dust}$ is resuspended dust-borne ^{10}Be
260 (all concentrations in atoms·m^{-3}). The dust-borne ^{10}Be must be removed to calculate
261 the corrected value $[^{10}Be]_{corr}$ (equation 3).

262 We measured atmospheric ^{7}Be and ^{10}Be values from different sites (Fig. 2a) and
263 different seasons (Fig. 2b), and used equation (1) to eliminate the influence of soil
264 dust on atmospheric ^{10}Be (Fig. 2c). The resuspension of terrestrial dust is controlled
265 by dryness and wind power (Zhang et al., 1997). Therefore, we chose representative
266 sampling sites with different atmospheric relative humidity and NDVI characteristics.
267 These sampling sites include ZW (h) in an arid and high-dust area, XA (b) and TY (i)
268 in semi-arid and low-humidity dusty regions, and CD (j), NN (k), LYG (l), and QL (g)
269 in humid and low-dust areas. These areas include typical geographic environments
270 such as deserts, coastal regions, humid inland regions, and areas prone to drought.

https://doi.org/10.5194/acp-2022-282
Preprint. Discussion started: 18 May 2022


Atmospheric Chemistry and Physics Discussions

271 The ^{7}Be concentration in the atmosphere is minimally disturbed by dust
272 (Yamagata et al., 2010). However, as shown in Fig. 2b, in three different seasons
273 (autumn, winter, and spring), ^{10}Be concentration fluctuations caused by the influence
274 of soil dust in different regions in the same season or at different times in the same
275 region are relatively large, which leads to large fluctuations in observed atmospheric
276 $^{10}Be/^{7}Be$ ratios (darker columns in Fig. 2c). These results show that the drier the area
277 is, the greater the short-term fluctuation of $^{10}Be/^{7}Be$ (Fig. 2c). Furthermore, Chen et al.
278 (2020b) pointed out that soil ^{10}Be in areas with less precipitation (< 1200 $mm \cdot a^{-1}$) is
279 more likely to be resuspended and not deposited in the surface soil. This conclusion
280 also shows once again that different amounts of resuspended dust can cause
281 fluctuations in observed atmospheric ^{10}Be concentrations.

282 Based on equation (1), after removing the soil dust contribution of each sampling
283 site (contamination rate shown as the black line, the bottom panel of Fig. 2c), the
284 corrected average $^{10}Be/^{7}Be$ ratios (colored horizontal lines, upper panel of Fig. 2c)
285 from each region are very similar. Among them, the XA $^{10}Be/^{7}Be$ correction ratio (b)
286 in winter (January) is larger than the average value, caused by local STE events. The
287 $^{10}Be/^{7}Be$ correction is relatively large, and the relative average value fluctuates
288 significantly in spring (April), because STE events frequently occur in spring. The
289 autumn-winter-spring trend in the average $^{10}Be/^{7}Be$ correction value is also consistent
290 with the seasonal variation of the $^{10}Be/^{7}Be$ ratio. Detailed ^{7}Be and ^{10}Be results are
291 given in Table S5.

292 To correct for dust-borne ^{10}Be concentrations in the atmosphere, the soil erosion

https://doi.org/10.5194/acp-2022-282
Preprint. Discussion started: 18 May 2022


Atmospheric Chemistry and Physics Discussions

conditions for each region need to be considered. Early studies made this correction based on Ca/Mg content (Brown et al., 1989;Mann et al., 2011) or U isotope composition (Monaghan et al., 1986). However, these methods overestimate the effects of dust and rely on assumptions that pose weak constraints on the dust composition (Graham et al., 2003). Zhang et al. (1994) pointed out that the Al provides an excellent means to calculate soil dust flux. Through simultaneous observations in different areas, we confirmed that the Al flux method (equation 1) proceeds an effective correction for atmospheric ^{10}Be. The corrected atmospheric ^{7}Be and ^{10}Be yielded ^{10}Be/^{7}Be records that reflected daily subsidence levels as an indicator of surface deposition processes. At the same time, the corrected atmospheric ^{10}Be provides a practical observation method for quantifying the ^{10}Be atmospheric input (Yi et al., 2019a), and to study East Asian summer monsoon rainfall changes and geomagnetic field changes (Kong et al., 2020).

https://doi.org/10.5194/acp-2022-282
Preprint. Discussion started: 18 May 2022

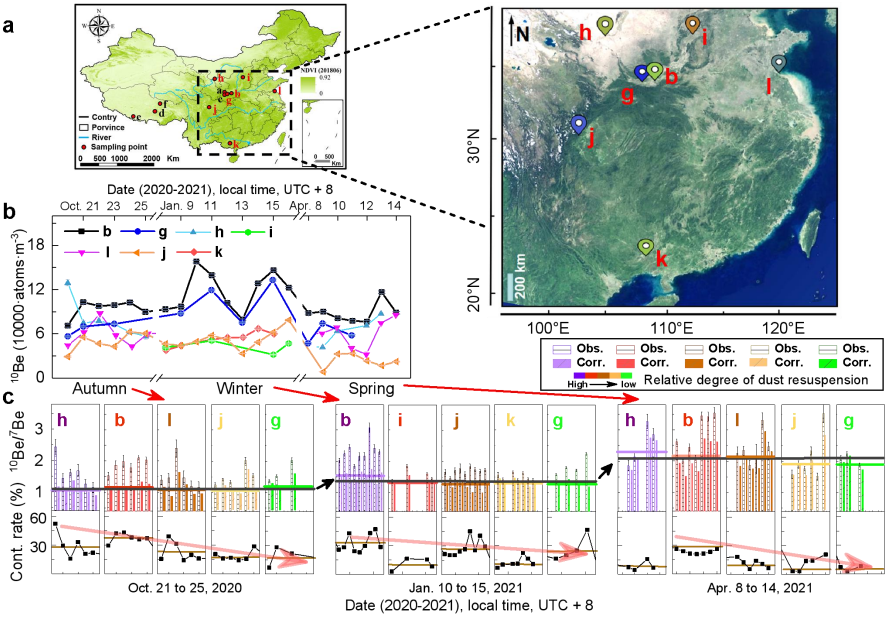

Fig. 2 Atmospheric ^{10}Be/^{7}Be observations and the impact of dust-borne ^{10}Be from each study region. (a). Sample site map with NDVI (modis.gsfc.nasa.gov/), and a satellite image of the entire study area (from © Google Maps). (b). Short-term fluctuations in surface aerosol ^{10}Be concentration during 3 different seasons at each sampling site. (c). Observed aerosol ^{10}Be/^{7}Be values (darker hollow columns), corrected ^{10}Be/^{7}Be values (brighter solid columns), and dust contribution (lower panel) before and after correction in 3 different seasons and regions. The horizontal lines represent average ^{10}Be/^{7}Be values after correction and the average value contribution rate from dust-borne ^{10}Be. The color of the columns from dark to light indicates that the relative resuspension amount of dust in various places in the same season gradually decreases. The arrows indicate trends.

3.3 Contribution of soil dust ^{10}Be in aerosols on the Loess Plateau

The observed aerosol ^{10}Be/^{7}Be ratios at the XA site during the dry period (blue

https://doi.org/10.5194/acp-2022-282
Preprint. Discussion started: 18 May 2022


Atmospheric Chemistry and Physics Discussions

line in Fig. 3a) deviate significantly from recent rainwater $^{10}Be/^{7}Be$ ratios (green line in Fig. 3a). In contrast, aerosol $^{10}Be/^{7}Be$ observations from the relatively low-dust QL site are consistent with rainwater $^{10}Be/^{7}Be$ (Fig. 3a). This result highlights the importance of correcting for resuspended dust-borne ^{10}Be.

The corrected aerosol $^{10}Be/^{7}Be$ ratios (red line in Fig. 3a) follow the rainfall $^{10}Be/^{7}Be$ trend. Corrected aerosol $^{10}Be/^{7}Be$ values from XA and QL are 0.91-3.73 and 0.93-2.56, respectively. The average annual contributions of resuspended dust-borne ^{10}Be for XA and QL were ~24% and ~12%, respectively (Fig. 3b; Table S3 and S4). The contribution of soil dust from the XA site is much higher than in low dust areas, such as New Zealand (11%) (Graham et al., 2003), Japan (~15%) (Yamagata et al., 2010), or Seville (10%) (Padilla et al., 2019).

The corrected aerosol $^{10}Be/^{7}Be$ ratios (red line in Fig. 3a) remove abrupt transient changes associated with dust-borne ^{10}Be (not STE events. This fluctuation is especially apparent at the XA site and is seen as "V"-shaped changes in the uncorrected record (enlarged view of Fig. 3a). The corrected $^{10}Be/^{7}Be$ ratios seen at the XA and QL sites are very similar, as would be expected once the dust-borne ^{10}Be has been removed. In addition, for atmospheric motion information that cannot be captured by rain samples when there is no precipitation, these corrected dry deposition $^{10}Be/^{7}Be$ ratios are an effective supplement.

https://doi.org/10.5194/acp-2022-282
Preprint. Discussion started: 18 May 2022

Atmospheric Chemistry and Physics Discussions

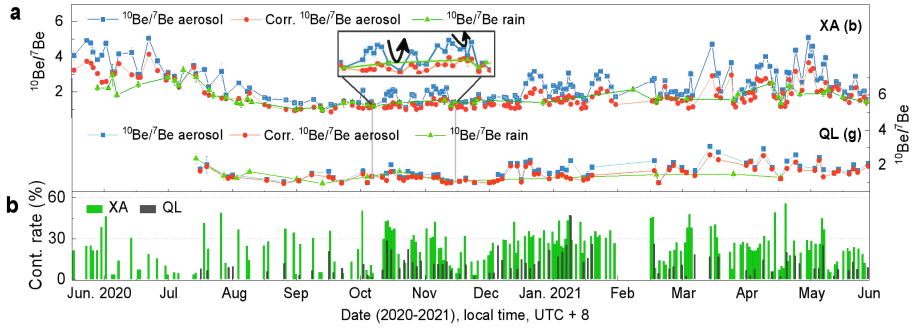

339

340 **Fig. 3** Correction of resuspended soil dust in aerosol ^{10}Be/^{7}Be on the Loess Plateau.
341 (a). Comparison of aerosol ^{10}Be/^{7}Be observations (blue) and corrected values (red),
342 with rainwater ^{10}Be/^{7}Be (green). (b). The contribution of soil dust ^{10}Be to aerosol
343 ^{10}Be/^{7}Be at the XA site (green) and QL site (black).

344

345 **3.4 Stratospheric air intrusions on the Loess Plateau and their contribution to**
346 **surface O_3**

347 As shown in Fig. 1a and 1b, high ^{7}Be and ^{10}Be concentrations in winter are
348 caused by the relatively long-term accumulation of surface aerosols during periods of
349 low precipitation (Yamagata et al., 2019). However, ^{10}Be/^{7}Be ratio change relatively
350 little in these cases (Fig. 1c). This is because the fixed production rate ratio and the
351 similar geochemical properties make ^{10}Be/^{7}Be resistant to air mass dilution at
352 different latitudes and rain removal. In addition, the large difference in the half-lives
353 of ^{7}Be and ^{10}Be and their fixed production rate lead to stratospheric ^{10}Be/^{7}Be ratios
354 that are significantly larger than in the troposphere. Thus, ^{10}Be/^{7}Be increases seen near
355 the surface air can be used to detect stratospheric air intrusion events.

356 Fig. 4a shows a distinct seasonal pattern in ^{10}Be/^{7}Be ratios from the XA and QL

https://doi.org/10.5194/acp-2022-282
Preprint. Discussion started: 18 May 2022


Atmospheric Chemistry and Physics Discussions

357 sites. This record is consistent with observational records (Jordan et al., 2003). Higher
358 $^{10}Be/^{7}Be$ ratios can indicate stratospheric air intrusion events superimposed on an
359 annual mean value of ~1 (Fig. 4). In spring and early summer (March to July), the
360 $^{10}Be/^{7}Be$ values reach a maximum of approximately 3 times higher than the annual
361 average. The increase is mainly affected by the Brewer-Dobson circulation in the
362 northern hemisphere (Butchart, 2014). The monthly $^{10}Be/^{7}Be$ variation box plot in the
363 upper right corner of Fig. 4a shows that the $^{10}Be/^{7}Be$ ratio between March and July is
364 relatively large and that the high-frequency positions are scattered. This indicates that
365 the intensity and frequency of stratospheric air intrusions during the "spring leakage"
366 of the atmosphere are higher. Conversely, the frequency and intensity of $^{10}Be/^{7}Be$
367 changes observed in other months are relatively scattered, indicating fewer but
368 distinct stratospheric air intrusion events during other periods of the year.

369 Sunlight is a natural prerequisite for the photochemical generation of O_3 at the
370 earth's surface (Kondratyev and Varotsos, 1996). The sunlight radiation follows a
371 symmetrical intensity law in the spring and autumn at the XA site (Fig. 4c). However,
372 surface O_3 concentrations at the XA site (Fig. 4b) are inconsistent with sunlight
373 radiation intensity (Fig. 4b blue area). This feature is consistent with the seasonal
374 increase in $^{10}Be/^{7}Be$. We suggest that surface O_3 concentration increases reflect an
375 influx of stratospheric O_3, indicated by frequent and relatively large changes in the
376 $^{10}Be/^{7}Be$. Similar results have been confirmed during spring in other regions using
377 ground-based lidar observations (Langford et al., 2009), airborne observations
378 (Weigel et al., 2012), and atmospheric models (Zhao et al., 2021). This also explains

https://doi.org/10.5194/acp-2022-282
Preprint. Discussion started: 18 May 2022

Atmospheric Chemistry and Physics Discussions

why surface O_3 concentrations are elevated in spring when the light intensity is comparable to that in autumn. With the arrival of summer, the light intensity gradually increases, and O_3 becomes dominated by the photochemical process at the surface (Fig. 4b).

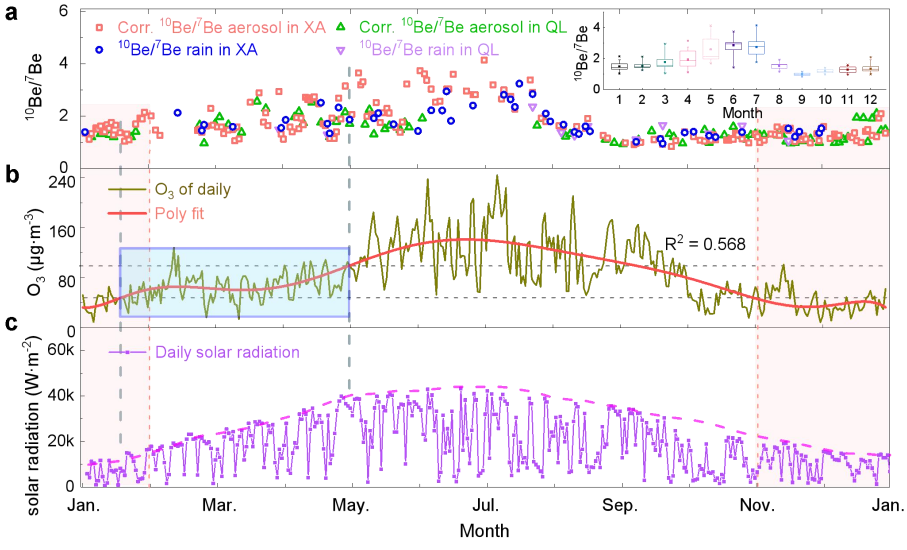

Fig. 4 The $^{10}Be/^{7}Be$ ratio response to seasonal stratospheric air intrusions, consistent with seasonal surface O_3 production on the Loess Plateau. (a). Seasonal $^{10}Be/^{7}Be$ variations. Inset shows a box plot (25%-75%) of monthly atmospheric $^{10}Be/^{7}Be$, with the 5%-95% whiskers, and minimum/maximum values indicated by asterisks. (b). Seasonal O_3 variations near the surface air at the XA site. Blue box indicates periods of high surface O_3 concentrations that are higher than expected from corresponding sunlight radiation intensities. (c). Seasonal sunlight radiation intensity at the XA site, with associated trend line (red dashed line).

https://doi.org/10.5194/acp-2022-282
Preprint. Discussion started: 18 May 2022


Atmospheric Chemistry and Physics Discussions

3.5 Evaluation of stratospheric O_3 intrusion with weak STE in winter

In addition to the strong "spring leakage" stratospheric air intrusion events that occur regularly every year, a number of relatively low-intensity stratospheric air intrusions are known to occur in other seasons. Li et al. (2021) pointed out that O_3 pollution during the winter haze season on the North China Plain is increasing. Ozone pollution caused by winter stratospheric air intrusions is particularly serious (Chen et al., 2020a). Although low-intensity and rapid stratospheric air intrusions are less significant than in summer, their adverse effects cannot be ignored. Our study shows that processes can be identified using ground-based $^{10}Be/^{7}Be$ measurements. Traditional gamma spectrometry is less well-suited to obtaining high-precision ^{7}Be measurements of low volume air samples. Furthermore, our approach makes it possible to make the daily measurements provide the requisite resolution necessary to understand the rapid and transient chemical reactions in the atmosphere (Zheng et al., 2011).

We observe frequent low but statistically significant ozone fluctuations in winter on the Loess Plateau (pink shaded area, Fig. 4). A comparison with our $^{10}Be/^{7}Be$ data, suggest low-intensity and rapid stratospheric air intrusions (November to January of the following year) at the XA site (Fig. 5). In the absence of stratospheric air intrusions, surface ozone shows a diurnal pattern with nighttime lows. However, when $^{10}Be/^{7}Be$ increases (blue vertical shaded area in Fig. 5a), surface O_3 concentrations increase (Fig. 5b). During these times, especially at night (shaded area in Fig. 5b), surface O_3 concentrations are not observed to decrease, and diurnal ozone pattern

https://doi.org/10.5194/acp-2022-282
Preprint. Discussion started: 18 May 2022


Atmospheric Chemistry and Physics Discussions

disappears. High O_3 concentrations are characteristics of the stratosphere (Kley et al., 2007). Therefore, these phenomena may be related to stratospheric air intrusions. Taken alone, the ozone trends can only be considered as indirect evidence for stratospheric air intrusions. However, considered alongside the $^{10}Be/^{7}Be$ results at the XA site, we interpret the covariation in winter to be related to rapid (1-3 days) stratospheric air intrusions.

A fixed relationship between O_3 and ^{7}Be during stratospheric air intrusions was proposed by Bazhanov and Rodhe (1997). Because $^{10}Be/^{7}Be$ avoids the interference of tropospheric variability on ^{7}Be concentrations, we substitute $\Delta(^{10}Be/^{7}Be)$ for the $\Delta^{7}Be$ to interpret surface ozone increases (ΔO_3). The ΔO_3 and $\Delta(^{10}Be/^{7}Be)$ values show a significantly positive correlation ($R^2 = 0.889$, $p < 0.01$. Fig. S4), providing a useful estimate of stratospheric ozone to the surface.

A surface O_3 record obtained by the above method is shown in Fig. 5c. We estimate that surface O_3 increased by 25.45% in the XA site during the winter of 2020/21. Chen et al. (2020a) used the hemisphere WRF-CMAQ model to find that the contribution of STE to surface O_3 in the winter of 2015 in eastern China was approximately 15%-21%. Stratospheric air intrusion in the Qinghai-Tibet Plateau of China has been shown to increase the O_3 concentrations in the troposphere by approximately 53% (Zhang et al., 2021). The influence of weather on surface O_3 in China varies by region, season, and year. It may be equivalent to or even more significant than the impact of changes in anthropogenic emissions, of which atmospheric motion has a significant contribution (Liu and Wang, 2020). O_3 brought

https://doi.org/10.5194/acp-2022-282
Preprint. Discussion started: 18 May 2022

Atmospheric Chemistry and Physics Discussions

437 by stratospheric air intrusion seriously affects the chemical balance of the
438 tropospheric atmosphere. For example, increased night-time O_3 (mainly input from
439 the stratosphere under STE) accelerates the conversion of NO_x to nitrate (Tang et al.,
440 2021), which has an important impact on atmospheric environmental pollution
441 process. In addition, this study proved that the relatively weak stratospheric air
442 intrusion process is randomly generated, which is an impact that needs to be
443 considered for the future surface O_3 concentration simulation.

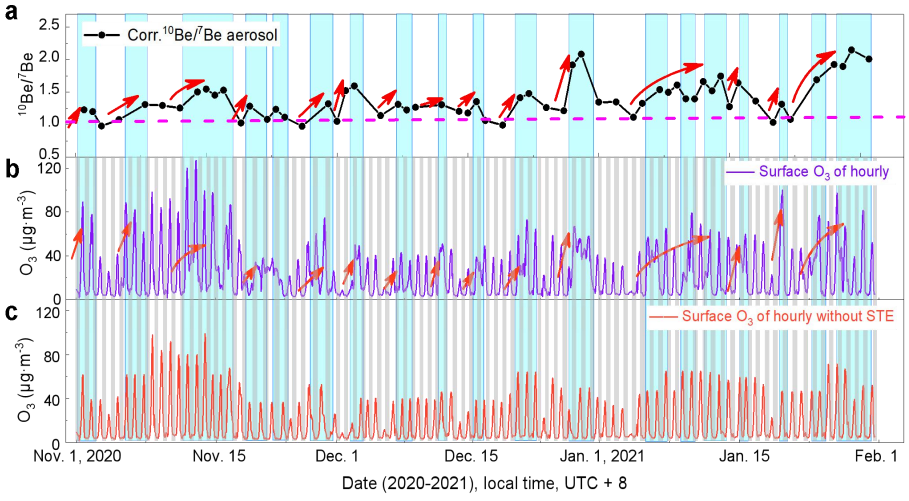

444

445 **Fig. 5** The influence of winter stratospheric air intrusions at the XA site and surface
446 O_3 compared with daily ^{10}Be/^{7}Be measurements. Aerosol ^{10}Be/^{7}Be ratio (a) and
447 surface O_3 concentrations (b) high-frequency variations at the XA site in winter. (c).
448 Surface O_3 concentrations after removing the contribution by stratospheric air
449 intrusions (see text). The purple line segment in Fig. 5a is the baseline of the ^{10}Be/^{7}Be
450 ratio when no STE occurs. The blue shaded areas indicate stratospheric air intrusions

https://doi.org/10.5194/acp-2022-282
Preprint. Discussion started: 18 May 2022


Atmospheric Chemistry and Physics Discussions

451 determined by $^{10}Be/^{7}Be$. Shaded areas in Fig. 5b and 5c indicate nighttime. Arrows
452 indicate trends.

453

454 **4 Conclusions**

455 STE is an important channel for transmitting atmospheric matters, particularly
456 low-intensity and frequent stratospheric air intrusion events that can quickly transmit
457 chemical matters to affect the environment. This work presents annual ground-based
458 $^{10}Be/^{7}Be$ records documenting stratospheric air intrusions. The main features of these
459 records include the following:

460 • High-sensitivity measurements (error ~ 1.5%) of ^{7}Be and ^{10}Be from single
461 targets prepared from aerosols (down to ~200 m^3 air) depending on AMS.

462 • Results in different regions confirm that Al content can be used to correct
463 resuspended dust-borne ^{10}Be in aerosol ^{10}Be.

464 • By measuring both rainwater and aerosols, $^{10}Be/^{7}Be$ measurements offer a
465 means of identifying stratospheric air intrusions throughout the year, with daily
466 resolution. The first of such records is presented herein, from the Loess Plateau of
467 China. We document $^{10}Be/^{7}Be$ records for 2020-2021 from two sites: 1) XA site -
468 rainwater $^{10}Be/^{7}Be$ was found to be 0.94-3.24, and the corrected aerosol $^{10}Be/^{7}Be$
469 range was found to be 0.91-3.73 after removal of the regional dust-borne component
470 (~24%); 2) QL site - rainwater $^{10}Be/^{7}Be$ was found to be 0.94-2.36, and the corrected
471 aerosol $^{10}Be/^{7}Be$ range was found to be 0.93-2.56 after the removal of the regional
472 dust-borne component (~12%).

https://doi.org/10.5194/acp-2022-282
Preprint. Discussion started: 18 May 2022


Atmospheric Chemistry and Physics Discussions

• Atmospheric $^{10}Be/^{7}Be$ on the Loess Plateau confirms that stratospheric air intrusions occur frequently and rapidly (1-3 days) throughout the year, with the strongest events in spring (March-July). These have a significant influence on surface ozone. It is shown by $\Delta(^{10}Be/^{7}Be)$ that even under weak stratospheric air intrusions in winter, the cumulative contribution to surface ozone at the XA site in 2020/21 is ~25%.

Data availability

The author declares that the main data supporting the results of this study can be found in the text and its supplementary materials.

Supplement

Supplementary information is available for this paper.

Author contribution statement

Xuke Liu finished the experiments, wrote the first version manuscript and analysed the data. Yunchong Fu conceived the original idea, performed AMS analysis and revised the initial manuscript. Xuke Liu and Yunchong Fu designed research roadmap. Li Zhang, Yanting Bi, and Guoqing Zhao designed chemical experiments and collected samples. Yunchong Fu assisted in AMS method development and supervised the research project. All the authors discussed the results and commented on the manuscript, and George S. Burr for revising manuscript language.

Competing interests

The authors declare no competing interests.

https://doi.org/10.5194/acp-2022-282
Preprint. Discussion started: 18 May 2022


Atmospheric Chemistry and Physics Discussions

Acknowledgements

We thank Weijian Zhou, Feng Xian, Peng Cheng, LuYuan Zhang, and Qi Liu for their help in the conducting experiments and discussing the results.

Financial support

This research has been supported by the National Natural Science Foundation of China (Grant No. 11975240), the Strategic Priority Research Program of Chinese Academy of Sciences (B) (Grant No. XDB40000000), and the Youth Innovation Promotion Association CAS (Grant No. Y2021108).

References

Adolphi, F., Muscheler, R., Svensson, A., Aldahan, A., Possnert, G., Beer, J., Sjolte, J., Bjorck, S., Matthes, K., and Thieblemont, R.: Persistent link between solar activity and Greenland climate during the Last Glacial Maximum, Nature Geoscience, 7, 662-666, 10.1038/ngeo2225, 2014.

Baylon, P. M., Jaffe, D. A., Pierce, R. B., and Gustin, M. S.: Interannual Variability in Baseline Ozone and Its Relationship to Surface Ozone in the Western US, Environmental Science & Technology, 50, 2994-3001, 10.1021/acs.est.6b00219, 2016.

Bazhanov, V., and Rodhe, H.: Tropospheric ozone at the Swedish mountain site Areskutan: Budget and trends, Journal of Atmospheric Chemistry, 28, 61-76, 10.1023/a:1005839313307, 1997.

Beck, J. W., Zhou, W. J., Li, C., Wu, Z. K., White, L., Xian, F., Kong, X. H., and An, Z.: A 550,000-year record of East Asian monsoon rainfall from Be-10 in loess, Science, 360, 877-+, 10.1126/science.aam5825, 2018.

Bhandari, N., Lal, D., and Rama: Stratospheric circulation studies based on natural and artificial radioactive tracer elements, Tellus, 18, 391-&, 10.1111/j.2153-3490.1966.tb00250.x, 1966.

https://doi.org/10.5194/acp-2022-282
Preprint. Discussion started: 18 May 2022


Atmospheric Chemistry and Physics Discussions

520 Brown, L., Stensland, G. J., Klein, J., and Middleton, R.: Atmospheric deposition of
521 Be-7 and Be-10, Geochimica Et Cosmochimica Acta, 53, 135-142,
522 10.1016/0016-7037(89)90280-9, 1989.
523 Butchart, N.: The Brewer-Dobson circulation, Reviews of Geophysics, 52, 157-184,
524 10.1002/2013rg000448, 2014.
525 Chen, L., Xing, J., Mathur, R., Liu, S. C., Wang, S. X., and Hao, J. M.: Quantification
526 of the enhancement of PM2.5 concentration by the downward transport of ozone
527 from the stratosphere, Chemosphere, 255, 10.1016/j.chemosphere.2020.126907,
528 2020a.
529 Chen, P., Yi, P., Czymzik, M., Aldahan, A., Ljung, K., Yu, Z. B., Hou, X. L., Zheng,
530 M. J., Chen, X. G., and Possnert, G.: Relationship between precipitation and
531 Be-10 and impacts on soil dynamics, Catena, 195, 10.1016/j.catena.2020.104748,
532 2020b.
533 Chham, E., Milena-Perez, A., Pinero-Garcia, F., Hernandez-Ceballos, M. A., Orza, J.
534 A. G., Brattich, E., El Bardouni, T., and Ferro-Garcia, M. A.: Sources of the
535 seasonal-trend behaviour and periodicity modulation of Be-7 air concentration in
536 the atmospheric surface layer observed in southeastern Spain, Atmospheric
537 Environment, 213, 148-158, 10.1016/j.atmosenv.2019.06.011, 2019.
538 Czymzik, M., Muscheler, R., Adolphi, F., Mekhaldi, F., Drager, N., Ott, F., Slowinski,
539 M., Blaszkiewicz, M., Aldahan, A., Possnert, G., and Brauer, A.: Synchronizing
540 Be-10 in two varved lake sediment records to IntCal13 C-14 during three grand
541 solar minima, Climate of the Past, 14, 687-696, 10.5194/cp-14-687-2018, 2018.
542 Fischer, H., Birk, M., Blom, C., Carli, B., Carlotti, M., von Clarmann, T., Delbouille,
543 L., Dudhia, A., Ehhalt, D., Endemann, M., Flaud, J. M., Gessner, R., Kleinert, A.,
544 Koopman, R., Langen, J., Lopez-Puertas, M., Mosner, P., Nett, H., Oelhaf, H.,
545 Perron, G., Remedios, J., Ridolfi, M., Stiller, G., and Zander, R.: MIPAS: an
546 instrument for atmospheric and climate research, Atmospheric Chemistry and
547 Physics, 8, 2151-2188, 10.5194/acp-8-2151-2008, 2008.
548 Graham, I., Ditchburn, R., and Barry, B.: Atmospheric deposition of Be-7 and Be-10

https://doi.org/10.5194/acp-2022-282
Preprint. Discussion started: 18 May 2022

549 in New Zealand rain (1996-98), Geochimica Et Cosmochimica Acta, 67, 361-373,
550 10.1016/s0016-7037(02)01092-x, 2003.
551 He, Y., Qiu, H. J., Song, J. X., Zhao, Y., Zhang, L. M., Hu, S., and Hu, Y. Y.:
552 Quantitative contribution of climate change and human activities to runoff
553 changes in the Bahe River watershed of the Qinling Mountains, China,
554 Sustainable Cities and Society, 51, 10.1016/j.scs.2019.101729, 2019.
555 Heikkila, U., Beer, J., Abreu, J. A., and Steinhilber, F.: On the Atmospheric Transport
556 and Deposition of the Cosmogenic Radionuclides (Be-10): A Review, Space
557 Science Reviews, 176, 321-332, 10.1007/s11214-011-9838-0, 2013.
558 Hernandez-Ceballos, M. A., Brattich, E., Lozano, R. L., and Cinelli, G.: Be-7
559 behaviour and meteorological conditions associated with Be-7 peak events in
560 Spain, Journal of Environmental Radioactivity, 166, 17-26,
561 10.1016/j.jenvrad.2016.03.019, 2017.
562 Hodnebrog, O., Myhre, G., Forster, P. M., Sillmann, J., and Samset, B. H.: Local
563 biomass burning is a dominant cause of the observed precipitation reduction in
564 southern Africa, Nature Communications, 7, 10.1038/ncomms11236, 2016.
565 Holton, J. R., Haynes, P. H., McIntyre, M. E., Douglass, A. R., Rood, R. B., and
566 Pfister, L.: Stratosphere-troposphere exchange, Reviews of Geophysics, 33,
567 403-439, 10.1029/95rg02097, 1995.
568 Jordan, C. E., Dibb, J. E., and Finkel, R. C.: Be-10/Be-7 tracer of atmospheric
569 transport and stratosphere-troposphere exchange, Journal of Geophysical
570 Research-Atmospheres, 108, 10.1029/2002jd002395, 2003.
571 Kley, D., Smit, H. G. J., Nawrath, S., Luo, Z., Nedelec, P., and Johnson, R. H.:
572 Tropical Atlantic convection as revealed by ozone and relative humidity
573 measurements, Journal of Geophysical Research-Atmospheres, 112,
574 10.1029/2007jd008599, 2007.
575 Kondratyev, K. Y., and Varotsos, C. A.: Global total ozone dynamics - Impact on
576 surface solar ultraviolet radiation variability and ecosystems .1. Global ozone
577 dynamics and environmental safety, Environmental Science and Pollution

https://doi.org/10.5194/acp-2022-282
Preprint. Discussion started: 18 May 2022


Atmospheric Chemistry and Physics Discussions

578 Research, 3, 153-157, 10.1007/bf02985523, 1996.
579 Kong, X. H., Zhou, W. J., Beck, J. W., Xian, F., Qiang, X. K., Ao, H., Wu, Z. K., and
580 An, Z. S.: Loess magnetic susceptibility flux: A new proxy of East Asian
581 monsoon precipitation, Journal of Asian Earth Sciences, 201,
582 10.1016/j.jseaes.2020.104489, 2020.
583 Lal, D., Malhotra, P. K., and Peters, B.: On the production of radioisotopes in the
584 atmosphere by cosmic radiation and their application to meteorology, Journal of
585 Atmospheric and Terrestrial Physics, 12, 306-328,
586 10.1016/0021-9169(58)90062-x, 1958.
587 Langford, A. O., Aikin, K. C., Eubank, C. S., and Williams, E. J.: Stratospheric
588 contribution to high surface ozone in Colorado during springtime, Geophysical
589 Research Letters, 36, 10.1029/2009gl038367, 2009.
590 Li, K., Jacob, D. J., Liao, H., Qiu, Y. L., Shen, L., Zhai, S. X., Bates, K. H., Sulprizio,
591 M. P., Song, S. J., Lu, X., Zhang, Q., Zheng, B., Zhang, Y. L., Zhang, J. Q., Lee,
592 H. C., and Kuk, S. K.: Ozone pollution in the North China Plain spreading into
593 the late-winter haze season, Proceedings of the National Academy of Sciences of
594 the United States of America, 118, 10.1073/pnas.2015797118, 2021.
595 Liu, X., Fu, Y., Wang, Q., Bi, Y., Zhang, L., Zhao, G., Xian, F., Cheng, P., Zhang, L.,
596 Zhou, J., and Zhou, W.: Unraveling the process of aerosols secondary formation
597 and removal based on cosmogenic beryllium-7 and beryllium-10, Science of the
598 total environment, 153293, 10.1016/j.scitotenv.2022.153293, 2022.
599 Liu, Y. M., and Wang, T.: Worsening urban ozone pollution in China from 2013 to
600 2017-Part 1: The complex and varying roles of meteorology, Atmospheric
601 Chemistry and Physics, 20, 6305-6321, 10.5194/acp-20-6305-2020, 2020.
602 Mann, M., Beer, J., Steinhilber, F., Abreu, J. A., Christl, M., and Kubik, P. W.:
603 Variations in the depositional fluxes of cosmogenic beryllium on short time
604 scales, Atmospheric Environment, 45, 2836-2841,
605 10.1016/j.atmosenv.2011.03.005, 2011.
606 Masarik, J., and Beer, J.: Simulation of particle fluxes and cosmogenic nuclide

https://doi.org/10.5194/acp-2022-282
Preprint. Discussion started: 18 May 2022


Atmospheric Chemistry and Physics Discussions

production in the Earth's atmosphere, Journal of Geophysical Research-Atmospheres, 104, 12099-12111, 10.1029/1998jd200091, 1999.

Monaghan, M. C., Krishnaswami, S., and Turekian, K. K.: The global-average production rate of Be-10, Earth and Planetary Science Letters, 76, 279-287, 10.1016/0012-821x(86)90079-8, 1986.

Padilla, S., Lopez-Gutierrez, J. M., Manjon, G., Garcia-Tenorio, R., Galvan, J. A., and Garcia-Leon, M.: Meteoric Be-10 in aerosol filters in the city of Seville, Journal of Environmental Radioactivity, 196, 15-21, 10.1016/j.jenvrad.2018.10.009, 2019.

Qiu, S. F., Zhu, Z. Y., Yang, T., Wu, Y., Bai, Y., and Ouyang, T. P.: Chemical weathering of monsoonal eastern China: implications from major elements of topsoil, Journal of Asian Earth Sciences, 81, 77-90, 10.1016/j.jseaes.2013.12.004, 2014.

Raisbeck, G. M., and Yiou, F.: Measurement of Be-7 by accelerator mass spectrometry, Earth and Planetary Science Letters, 89, 103-108, 10.1016/0012-821x(88)90035-0, 1988.

Randel, W. J., Park, M., Emmons, L., Kinnison, D., Bernath, P., Walker, K. A., Boone, C., and Pumphrey, H.: Asian Monsoon Transport of Pollution to the Stratosphere, Science, 328, 611-613, 10.1126/science.1182274, 2010.

Shen, C. D., Beer, J., Kubik, P. W., Sun, W. D., Liu, T. S., and Liu, K. X.: Be-10 in desert sands, falling dust and loess in China, Nuclear Instruments & Methods In Physics Research Section B-Beam Interactions with Materials and Atoms, 268, 1050-1053, 10.1016/j.nimb.2009.10.095, 2010.

Sudo, K., Takahashi, M., and Akimoto, H.: Future changes in stratosphere-troposphere exchange and their impacts on future tropospheric ozone simulations, Geophysical Research Letters, 30, 10.1029/2003gl018526, 2003.

Tan, Y. L., Qiao, Y. S., Zhao, Z. Z., Wang, Y., Qi, L., Fu, J. L., Liu, Z. X., Yao, H. T., Wang, S. B., and Jiang, F. C.: Geochemical Characteristics of Eolian Deposits in

https://doi.org/10.5194/acp-2022-282
Preprint. Discussion started: 18 May 2022

the Chengdu Plain of Sichuan Province and the Implications for Provenance, Acta Geologica Sinica-English Edition, 87, 1712-1723, 10.1111/1755-6724.12171, 2013.

Tang, G. Q., Wang, Y. H., Liu, Y. S., Wu, S., Huang, X. J., Yang, Y., Wang, Y. M., Ma, J., Bao, X. L., Liu, Z. R., Ji, D. S., Li, T. T., Li, X., and Wang, Y. S.: Low particulate nitrate in the residual layer in autumn over the North China Plain, Science of the Total Environment, 782, 10.1016/j.scitotenv.2021.146845, 2021.

Tiessen, C., Bemmerer, D., Rugel, G., Querfeld, R., Scharf, A., Steinhauser, G., and Merchel, S.: Accelerator mass spectrometry (AMS) for beryllium-7 measurements in smallest rainwater samples, Journal of Radioanalytical and Nuclear Chemistry, 319, 965-973, 10.1007/s10967-018-6371-6, 2019.

Weigel, K., Hoffmann, L., Gunther, G., Khosrawi, F., Olschewski, F., Preusse, P., Spang, R., Stroh, F., and Riese, M.: A stratospheric intrusion at the subtropical jet over the Mediterranean Sea: air-borne remote sensing observations and model results, Atmospheric Chemistry and Physics, 12, 8423-8438, 10.5194/acp-12-8423-2012, 2012.

Xiong, S. F., Ding, Z. L., Zhu, Y. J., Zhou, R., and Lu, H. J.: A similar to 6 Ma chemical weathering history, the grain size dependence of chemical weathering intensity, and its implications for provenance change of the Chinese loess-red clay deposit, Quaternary Science Reviews, 29, 1911-1922, 10.1016/j.quascirev.2010.04.009, 2010.

Yamagata, T., Sugihara, S., Morinaga, I., Matsuzaki, H., and Nagai, H.: Short term variations of Be-7, Be-10 concentrations in atmospheric boundary layer, Nuclear Instruments & Methods In Physics Research Section B-Beam Interactions with Materials and Atoms, 268, 1135-1138, 10.1016/j.nimb.2009.10.117, 2010.

Yamagata, T., Nagai, H., Matsuzaki, H., and Narasaki, Y.: Decadal variations of atmospheric Be-7 and Be-10 concentrations between 1998 and 2014 in Japan, Nuclear Instruments & Methods In Physics Research Section B-Beam Interactions with Materials and Atoms, 455, 265-270,

https://doi.org/10.5194/acp-2022-282
Preprint. Discussion started: 18 May 2022

10.1016/j.nimb.2018.12.029, 2019.

Yi, P., Yu, Z., Chen, P., Aldahan, A., Hou, X., Fan, Y., Chen, L., Possnert, G., Muscheler, R., Zhou, W., Sudicky, E., Schwartz, F., and Murad, A.: Late Holocene pathway of Asian Summer Monsoons imprinted in soils and societal implications, Quaternary Science Reviews, 215, 35-44, 10.1016/j.quascirev.2019.05.002, 2019a.

Yi, P., Yu, Z. B., Chen, P., Aldahan, A., Hou, X. L., Fan, Y. K., Chen, L., Possnert, G., Muscheler, R., Zhou, W. J., Sudicky, E., Schwartz, F., and Murad, A.: Late Holocene pathway of Asian Summer Monsoons imprinted in soils and societal implications, Quaternary Science Reviews, 215, 35-44, 10.1016/j.quascirev.2019.05.002, 2019b.

Zhang, J. Q., Li, D., Bian, J. C., and Bai, Z. X.: Deep stratospheric intrusion and Russian wildfire induce enhanced tropospheric ozone pollution over the northern Tibetan Plateau, Atmospheric Research, 259, 10.1016/j.atmosres.2021.105662, 2021.

Zhang, L., and Fu, Y. C.: Preliminary study of Be-10/Be-7 in rainwater from Xi'an by Accelerator Mass Spectrometry, Chinese Physics C, 41, 10.1088/1674-1137/41/1/018201, 2017.

Zhang, X. Y., An, Z. S., Chen, T., Zhang, G. Y., Arimoto, R., and Ray, B. J.: Late Quaternary Records of the Atmospheric Input of Eolian Dust to the Center of the Chinese Loess Plateau, Quaternary Research, 41, 35-43, 10.1006/qres.1994.1004, 1994.

Zhang, X. Y., Arimoto, R., and An, Z. S.: Dust emission from Chinese desert sources linked to variations in atmospheric circulation, Journal of Geophysical Research-Atmospheres, 102, 28041-28047, 10.1029/97jd02300, 1997.

Zhao, K. H., Hu, C., Yuan, Z. B., Xu, D. N., Zhang, S., Luo, H. H., Wang, J. T., and Jiang, R. S.: A modeling study of the impact of stratospheric intrusion on ozone enhancement in the lower troposphere over the Hong Kong regions, China, Atmospheric Research, 247, 10.1016/j.atmosres.2020.105158, 2021.

https://doi.org/10.5194/acp-2022-282
Preprint. Discussion started: 18 May 2022


Atmospheric Chemistry and Physics Discussions

694 Zheng, X. D., Wan, G. J., and Tang, J.: Source characteristics of O3 and CO2 at Mt.
695 Waliguan Observatory, Tibetan Plateau implied by using Be-7 and Pb-210,
696 Science China-Earth Sciences, 54, 550-560, 10.1007/s11430-010-4121-x, 2011.
697 Zhou, W. J., Chen, M. B., Xian, F., Song, S. H., Wu, Z. K., Jull, A. J. T., and Liu, W.
698 G.: The mean value concept in mono-linear regression of multi-variables and its
699 application to trace studies in geosciences, Science In China Series D-Earth
700 Sciences, 50, 1828-1834, 10.1007/s11430-007-0123-8, 2007.

701